Geophysical Research Letters

RESEARCH LETTER
10.1029/2025GL118283

The Role of Normal Stress and Shear Stress Heterogeneity in the Inferred Depth-Independence of Stress Drop

Minghan Yang[1], **Valère Lambert**[1], **and Emily E. Brodsky**[1]

[1]Department of Earth and Planetary Science, University of California Santa Cruz, Santa Cruz, CA, USA

Key Points:

- Higher normal stress decreases earthquake nucleation size, promoting an increased range of rupture sizes and shear stress heterogeneity
- As fault models increasingly exceed nucleation sizes under higher normal stress, rupture behaviors reflect more heterogeneous prestress
- Stress drop dependence on normal stress is weaker than linear and fit by a sublinear power law, partly explaining the depth-independence

Supporting Information:

Supporting Information may be found in the online version of this article.

Correspondence to:

M. Yang,
myang122@ucsc.edu

Citation:

Yang, M., Lambert, V., & Brodsky, E. E. (2026). The Role of normal stress and shear stress heterogeneity in the inferred depth-independence of stress drop. *Geophysical Research Letters*, *53*, e2025GL118283. https://doi.org/10.1029/2025GL118283

Received 18 JUL 2025
Accepted 13 JAN 2026

Abstract Earthquake stress drops are inferred to be independent of source depth, contradicting linear scaling predictions for earthquakes as frictional stick-slip instabilities that assume increasing fault normal stress due to overburden. Here, we examine the scaling between averaged stress drops and increasing normal stress for simulated earthquake sequences in continuum rate-and-state fault models. The models produce a weaker dependence of stress drop on normal stress than the linearity of simple friction, which can be well-fit by a sublinear power-law. This result is more prominent when the fault dimension is much larger than nucleation scales. In such cases, the averaged behavior of ruptures is dominated by rupture propagation conditions, reflecting more heterogeneous shear stress conditions. As natural faults can be considerably larger than the smallest earthquakes they host, such a weaker scaling between averaged rupture conditions and normal stress may partially explain the lack of an inferred depth-dependence of earthquake stress drops.

Plain Language Summary Earthquakes release stress. Observations suggest that stress drop during an earthquake does not depend on the depth at which earthquakes occur. This observation is confusing because earthquakes are frictional slip events and a fundamental property of friction is that the shear stress in the direction of sliding is proportional to the fault normal stress. The fault normal stress is expected to increase with depth given the increasing weight of the overlying rock, which would predict an increase in stress drop. Here, we explore this conundrum using computer simulations of earthquake ruptures in fault models with increasing normal stress. We find the scaling between stress drop and normal stress in our models follows a sublinear power-law scaling that is weaker than linear predictions from simplified friction models. This effect is more pronounced at depth as the size of the smallest earthquakes in each model decreases with increasing normal stress, resulting in a wider range of rupture sizes that occur over more heterogeneous shear stress conditions. As natural faults can be much larger than the smallest earthquakes they host, the weaker scaling observed in our models may partially explain the lack of an inferred depth dependence of earthquake stress drop.

1. Introduction

The absolute values of the shear stress released during an earthquake serve as a crucial parameter for estimating the intensity of ground motions (Abercrombie, 2021; Oth et al., 2017) and thus, for seismic hazard assessment (Trugman & Shearer, 2017). Stress drop reflects the shear stress changes on a fault before and after an earthquake rupture, with the strain energy change from released stress promoting rupture propagation. Understanding how stress drop depends on the rupture process is important for interpreting seismological observations in terms of the underlying earthquake physics.

Stress drop is routinely inferred from the duration and amplitude of radiated seismic waves (Brune, 1970; Kaneko & Shearer, 2015). Seismological estimates of stress drop are largely independent of the earthquake depth. This depth-independence is seen in systematic analyses of earthquakes from global and regional catalogs (Allmann & Shearer, 2007, 2009; Shearer et al., 2006, 2022). While some studies suggest that stress drops increase with earthquake source depth (Huang et al., 2017; Trugman, 2020), such a dependence may disappear after accounting for depth-dependent attenuation effects and rupture velocity (Abercrombie & Baltay, 2025; Abercrombie et al., 2021; Bilek & Lay, 1999; Bindi et al., 2023; Lay et al., 2012; Shearer et al., 2006). Even at extreme depths, the ratio of slip to rupture length (strain drop) does not systematically change with overburden (Vallée, 2013).

If fault normal stress increases with depth due to rock overburden, the inferred depth-independence of seismological stress drop and the amount of slip for a given rupture area suggest that they are also independent of normal stress. This observation conflicts with conceptual models of earthquake ruptures as frictional sliding events, such

as the single degree-of-freedom slider-block model (Brace & Byerlee, 1966). A fundamental property of Coulomb friction is that the shear stress τ along an interface is proportional to the normal stress σ (Scholz, 1998):

$$\tau = \sigma\mu \tag{1}$$

As a result, the change in shear stress reflected in the earthquake geometric aspects and associated seismological stress drop is expected to be directly influenced by normal stress. For example, in a slider-block governed by standard rate-and-state friction (Dieterich, 1979; Ruina, 1983), the stress drop $\Delta\tau$ is proportional to normal stress σ expressed as:

$$\Delta\tau = \sigma\left[(b-a)\log\left(\frac{V_{\mathrm{dyn}}}{V_{\mathrm{pl}}}\right)\right] \tag{2}$$

where a and b represent the direct and evolution effects respectively, V_{dyn} is the dynamic level of slip rate, and V_{pl} is the tectonic loading rate.

Several hypotheses have been proposed to explain the inferred depth-independence of earthquake stress drops. One explanation is that fault zones experience increasing pore fluid overpressure with increasing depth, such that the effective normal stress, defined as the difference between normal stress and pore pressure, is approximately constant at different depths (Liu & Rice, 2005). However, in situ measurements of pore fluid pressure remain unavailable at seismogenic depths.

An alternative hypothesis is that natural faults experience enhanced dynamic weakening at seismic slip rates, which can create nonlinear feedbacks between shear stress and normal stress during dynamic rupture (Rice, 2006). The efficiency of some dynamic weakening mechanisms, such as the thermal pressurization of pore fluids, depends on the absolute level of shear stress. Consequently, higher shear stresses due to higher normal stress can promote more efficient fault weakening and rupture propagation into regions of lower shear stress (Lambert, Lapusta, & Perry, 2021; Noda et al., 2009; Perry et al., 2020). This in turn results in larger ruptures propagating over lower average prestress conditions (Lambert, Lapusta, & Perry, 2021; Perry et al., 2020), with consequently lower average stress drops than models with the same normal stress but without dynamic weakening.

A third potential explanation is motivated by laboratory experiments that observe normal stress-independent stress drops for frictional slip events without any extreme conditions like dynamic weakening (Steinhardt & Brodsky, 2025; Steinhardt et al., 2023). Steinhardt et al. (2023) find that stress drops calculated for slip events along a frictional interface do not depend on the normal load when the samples are sufficiently large such that ruptures are confined within the boundaries of the sample interface. This normal stress independence disappears when the size of the frictional interface is reduced. Prior studies found that stress drops in laboratory slip events did depend on the normal load, however such studies largely considered unconfined slip events that rupture the entire sample due to high stiffness of rock samples (Beeler et al., 2012; Okubo & Dieterich, 1984). In aggregate, the observations suggest rupture confinement may play a role in the normal stress dependence of averaged stress drop.

Motivated by the experiments of Steinhardt et al. (2023), here we explore the hypothesis that the averaged stress drop of frictional ruptures may exhibit a weaker dependence on normal stress compared to standard expectations of linear scaling from Coulomb friction due to the averaging of different stress conditions for areas of rupture nucleation and propagation (Lambert, Lapusta, & Faulkner, 2021; Perry et al., 2020) and stress field heterogeneity. We examine the scaling between normal stress and averaged stress drop in simulated ruptures using numerical simulations of sequences of earthquakes and aseismic slip in fault models governed by standard rate-and-state friction. While we prescribe uniform parameters along the seismogenic portion of the fault, the shear stress field can become highly heterogeneous over earthquake sequences. We discuss the relationship between the evolution of the shear stress distribution and a non-dimensional quantity referred to as the instability ratio and show that stress history due to prior fault slip facilitates rupture propagation into low stress regions, resulting in lower stress drops for ruptures that grow much larger than the nucleation scale. We find a power-law-like dependence of stress drop on normal stress that is weaker than the linear scaling predictions from Coulomb friction. Finally, we connect the scaling predictions of the models to natural faults.

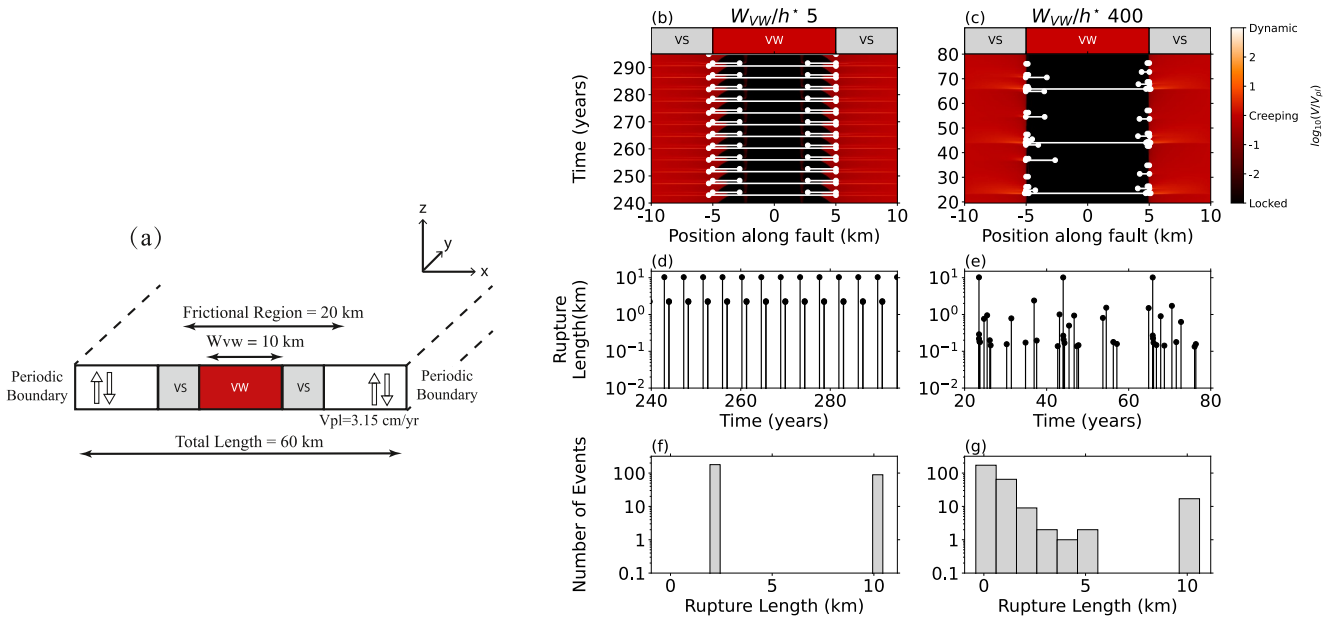

Figure 1. (a) Model configuration and (b–g) examples of simulated earthquake sequences. (b, c) Fault slip rate normalized by the long-term loading rate (log-scale) illustrates sequences of seismic events with intermittent periods of locking (black) within the Velocity-Weakening (VW) region, with loading due to aseismic slip around the long-term loading rate (red) in the surrounding Velocity-Strengthening (VS) regions. Horizontal white solid lines depict the ruptured length of simulated earthquakes. (d, f) Time series and histograms of simulated events with varying rupture lengths for the fault model shown in (b) with lower instability ratio. (e, g) Time series and histograms showing increased variability in timing and rupture lengths for events in the fault model shown in (c) with higher instability ratio.

2. Method and Model Setup

We employ the numerical methodology of Lapusta et al. (2000) to simulate all stages of earthquake sequences, including spontaneous earthquake nucleation, rupture propagation, postseismic deformation, and interseismic loading. We consider a one-dimensional (1D) fault embedded in a two-dimensional (2D) uniform, isotropic elastic medium (Figure 1) loaded with a long-term tectonic loading rate V_{pl} (Table S1 in Supporting Information S1). The fault is governed by the standard Dieterich-Ruina rate-and-state friction law, with the frictional state evolution governed by the aging law (Dieterich, 1979). Our fault models contain a 10-km long region of velocity-weakening friction, where ruptures nucleate and mostly propagate, surrounded by regions of velocity-strengthening friction, which promotes more stable sliding (Figure 1a). We use the quasi-dynamic approximation for inertial effects during earthquake rupture propagation (Rice, 1993) to mitigate the computational expense associated with calculating the dynamic wave-mediated stress transfer (Lapusta et al., 2000). Further details of the method can be found in Text S1 of Supporting Information S1.

Unstable slip can only accelerate into earthquake ruptures if the size of the velocity-weakening region W_{vw} is larger than a critical nucleation scale h^*. Several estimates of the critical nucleation scale have been proposed (Text S1 in Supporting Information S1), including the estimate of Rubin and Ampuero (2005) based on an analogy to a critical crack size for dynamic fracture:

$$h^* = \frac{2}{\pi}\frac{b}{(b-a)^2}\frac{G\mathrm{D_{RS}}}{\sigma} \tag{3}$$

where G is the shear modulus and D_{RS} is the characteristic slip distance. The estimate of Rubin and Ampuero (2005) represents the minimum size of a slipping region that releases enough stored elastic energy to radiate seismic waves and characterizes the size of the smallest earthquake ruptures occurring in our models.

Prior studies of continuum fault models and meter-scale laboratory experiments, have shown that fault slip behavior can depend on a non-dimensional quantity referred to as the instability ratio R_I, defined as the ratio of length of the velocity-weakening region W_{vw} to the nucleation scale (Barbot, 2019; Cattania, 2019; Lambert & Lapusta, 2021; Lapusta & Rice, 2003; Song & McLaskey, 2024; Wu & Chen, 2014):

$$R_I = \frac{W_{\text{vw}}}{h^*} \quad (4)$$

Earthquakes nucleate in fault models when R_I exceeds 1. W_{vw} provides an estimate of the largest earthquakes that occur when R_I is larger than 1, and as R_I becomes much larger than 1, a wider range of rupture sizes can appear in simulated earthquake sequences.

In this study, we explore the scaling of stress drop in fault models with increasing normal stress. We fix all parameters except for the fault normal stress, which varies from 5 to 200 MPa, corresponding to instability ratios R_I from ∼20 to ∼800 (Table S1 in Supporting Information S1). We also examine models with fixed instability ratio by increasing the characteristic slip distance D_{RS} and normal stress in a consistent manner such that D_{RS}/σ and hence R_I remains constant.

We define the ruptured region of simulated events as fault regions over which the slip rate exceeds a threshold (Text S1 in Supporting Information S1). We calculate the stress drop distribution along the ruptured area as the difference between the initial (prestress) and final shear stress distributions for each rupture, defined by the time when the maximum slip rate along the fault exceeds or drops below the velocity threshold, respectively. We compute moment-based averaged stress drop estimates using the weighting presented by Noda et al. (2013) and find that modest differences in velocity threshold and the averaging method do not change the main results of this work (Text S2 and Figures S1–S4 in Supporting Information S1). Note that in the present study the rigidity is constant and thus stress drop and strain drop have the same systematics.

3. Results

3.1. Increasing Rupture and Prestress Variability With Increasing Normal Stress and Instability Ratio

As the fault normal stress and instability ratio R_I increase across our models, the sequences of slip events exhibit increasing variability, including the range and frequency distribution of event sizes (Figure 1; Wu & Chen, 2014; Cattania, 2019; Barbot, 2019; Lambert & Lapusta, 2021). Fault models with lower normal stress, and hence lower R_I, exhibit simpler slip sequences with characteristic earthquakes that occur with regular interevent times (Figures 1b, 1d, and 1f). In contrast, the earthquake sequence for a model with a higher normal stress and R_I exhibits a more complex pattern of partial ruptures with varying rupture sizes (Figures 1c, 1e, and 1g). The variability in slip sequences with increasing normal stress and instability ratio R_I arises because the nucleation scale, and hence the size of the smallest earthquakes that occur within the models, decreases with increasing normal stress (e.g., pink vs. green circles in Figure 2a). As the range of possible rupture sizes increases with the instability ratio, the shear stress distributions become more heterogeneous given the history of slip and stress changes in prior events, resulting in a broader distribution of the averaged prestress conditions across different ruptures (Figure 2b).

As in prior studies (Lambert, Lapusta, & Faulkner, 2021; Perry et al., 2020), our models exhibit a mild decrease in stress drop with increasing rupture length (Figure 2a), which appears to contradict the seismologically inferred magnitude invariance of stress drop (Kanamori & Anderson, 1975). However, the dependence is weak for our models with a reduction by a factor of 4 for two orders of magnitude increase in rupture length (Figure 2a). As seismological estimates of stress drop are scattered over several orders of magnitude (Abercrombie et al., 2025), the mild decrease in stress drop with rupture length observed in our models may not be discernible within observational variations.

Our models suggest that the relationship between the average fault prestress and fault normal stress differs with the size of simulated ruptures with respect to their nucleation region, which is influenced by R_I (Figure 2). Let us consider two representative events that have a similar rupture length from two models with 25 and 100 MPa normal stress and differing R_I (Figures 3a and 3b). The normal stress between the fault models differs by a factor of 4. However, the stress drop (2.4 MPa) from the model with 100 MPa normal stress is less than 3 times higher than that (0.9 MPa) from the model with 25 MPa normal stress, suggesting the average stress drop of comparable rupture sizes does not scale linearly with normal stress across our models.

For standard rate-and-state friction, ruptures nucleate in regions where the shear stress is close to the local quasi-static fault strength (Lambert, Lapusta, & Faulkner, 2021), around an apparent friction (or shear stress divided by

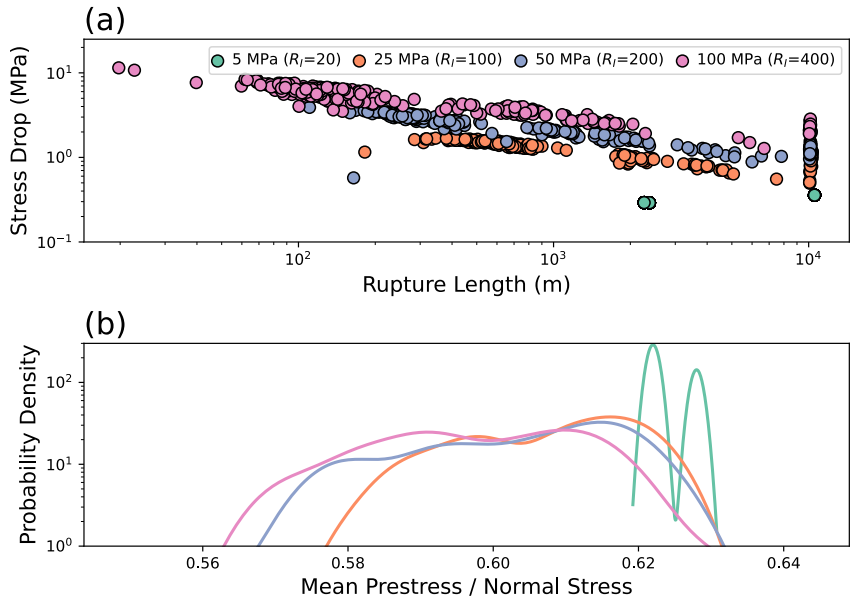

Figure 2. (a) Average stress drops for ruptures with varying rupture lengths form models with increasing normal stress and instability ratio. (b) Distribution of averaged rupture prestress normalized by fault normal stress across ruptures in each fault model, illustrating a wider range of average prestress conditions taking part in simulated ruptures for models with increasing normal stress and instability ratio.

normal stress) of 0.63 in our models. The shear resistance weakens with slip to an essentially fixed dynamic resistance level (an apparent friction around 0.55). The quasi-static strength and dynamic resistance vary directly with normal stress (Equations S14 and S15 and Text S1 in Supporting Information S1), predicting an increase in local stress drop with normal stress, which does indeed occur around the nucleation region where the prestress levels are near the quasi-static strength.

As ruptures propagate, the shear stress in slipping regions is redistributed in part to neighboring regions through elastic stress transfer, which facilitates rupture propagation into regions with lower shear stress conditions below the quasi-static strength and can result in more heterogeneous shear stress distributions as the range of rupture sizes increases (Figures 3e and 3f). The residual stress from prior smaller events assists the propagation of subsequent larger ruptures into regions of low shear stress. For example, the prestress at the tail end of the rupture in the fault model with 100 MPa normal stress and higher R_I is closer to the final stress (red vs. blue lines in Figure 3f) compared to that of the rupture with 25 MPa normal stress and lower R_I (Figure 3e), which is reflected in the shift of the normalized prestress distribution to lower relative shear stress (Figure 3g). Rupture propagation over these relatively lower prestress levels is facilitated by rupture acceleration due to the residual stress from a prior smaller rupture (Figures 3d and 3f). Given comparable normalized dynamic resistance levels (i.e., final stress, red lines in Figures 3e and 3f), the lower normalized prestress conditions from the model with higher normal stress and R_I (Figure 3g) suggests a milder dependence of the stress drop distribution on normal stress than simple linear Coulomb scaling.

3.2. Scaling of Stress Drop With Normal Stress in Continuum Fault Models With Rate-And-State Friction

Here, we examine how the average stress drop for simulated ruptures scales with increasing normal stress and instability ratio R_I. We compare our results with the linear scaling defined by Equation 2 for the reference. First, we consider models where the R_I is fixed by increasing the characteristic slip distance (D_{RS}) along with increasing normal stress. As the distribution of rupture sizes, and prestress heterogeneity, can be characterized by R_I, the evolving shear stress distributions may be expected to scale comparably across different normal stresses. Indeed, we find that the averaged stress drop, taken across ruptures within a given fault model, scales nearly linearly with fault normal stress across models with fixed R_I (Figures 4a and 4b), consistent with standard predictions (dashed reference line for linear scaling).

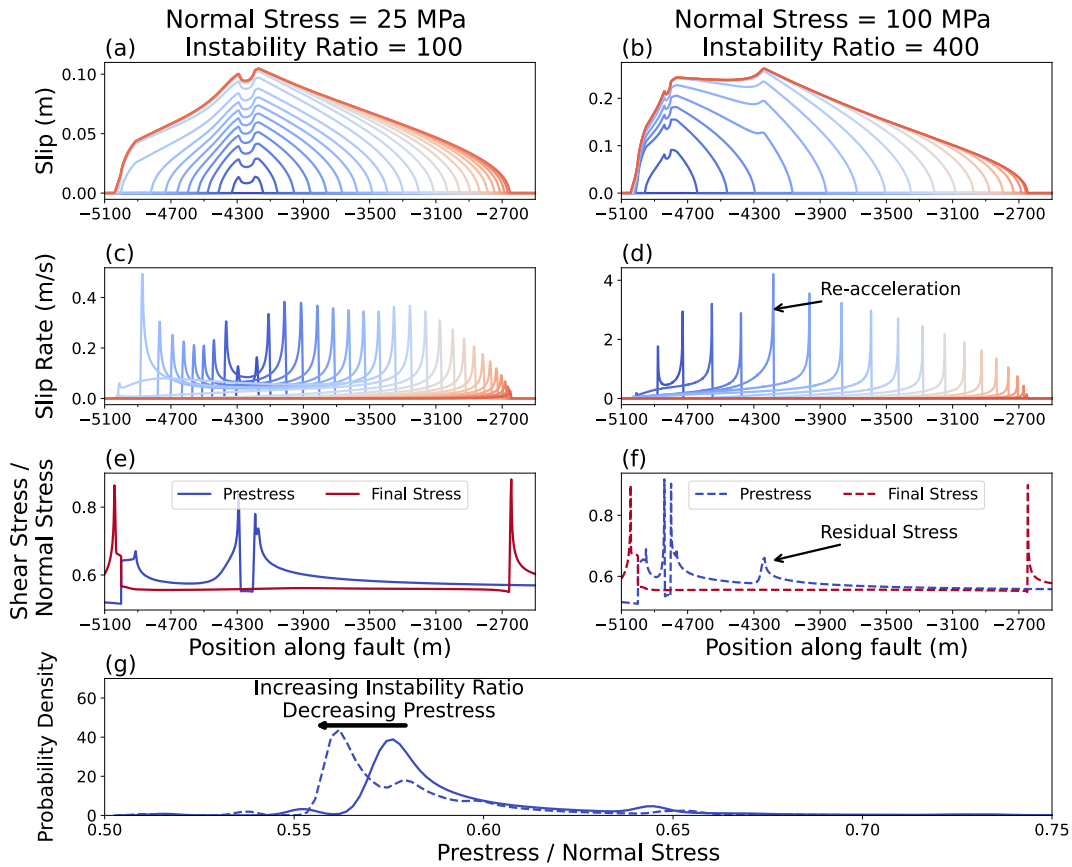

Figure 3. Two representative events with similar event size from models with normal stress of 25 and 100 MPa. (a, b) Slip contours are plotted every 0.166 s with respect to the onset of each event. (c, d) Contours of slip rate illustrating the acceleration and arrest of the ruptures with the same interval in a and b. (e, f) Distributions of fault shear stress, normalized by normal stress, before (prestress, blue) and after (final stress, red) each event. (g) The probability density function of the prestress fields, normalized by fault normal stress, in (e, f).

We next consider fault models where all fault parameters are fixed except for increasing normal stress, allowing R_I to increase with normal stress. The scaling between the average stress drop of all events and normal stress across our fault models is weaker than the reference linearity when the instability ratio R_I also increases with normal stress (Figures 4c and 4d). We find that the dependence of stress drop on normal stress - quantified as the derivative with respect to normal stress - varies with R_I, which is stronger at smaller R_I and weaker at larger R_I. This scaling can be well-fit by a power law with an exponent less than one (the red line in Figures 4c and 4d). The modeled average stress drops still exhibit a dependence on the fault normal stress. However, an exponent less than one in the power law implies that the dependence decreases asymptotically approaching zero at very large R_I (Figures 4c and 4d).

The red dots in Figure 4c are the averaged stress drop values across all rupture sizes in each model. If we examine only ruptures that are considerably larger than their nucleation scale, the scaling with fault normal stress is even weaker (blue dots in Figures 4c and 4d). The averaged rupture behavior for events that grow larger than the nucleation region is increasingly dominated by the conditions for rupture propagation (Lambert, Lapusta, & Faulkner, 2021), which reflect more heterogeneous prestress conditions that depend on the complex history of prior fault slip, and are generally lower than the quasi-static strength (Figure 3). As the nucleation scale decreases in models with higher normal stress, the fraction of ruptures that is larger than the nucleation scale increases. These larger ruptures have distributions of the prestress that is less concentrated around the quasi-static strength (Figure 3) and the resulting distribution of stress drops show a weaker correlation with normal stress. In contrast, the stress drops for the smallest events in the models increase nearly proportionally with normal stress. This effect is shown by the green dots in Figures 4c and 4d where for events with rupture lengths within 10 times the

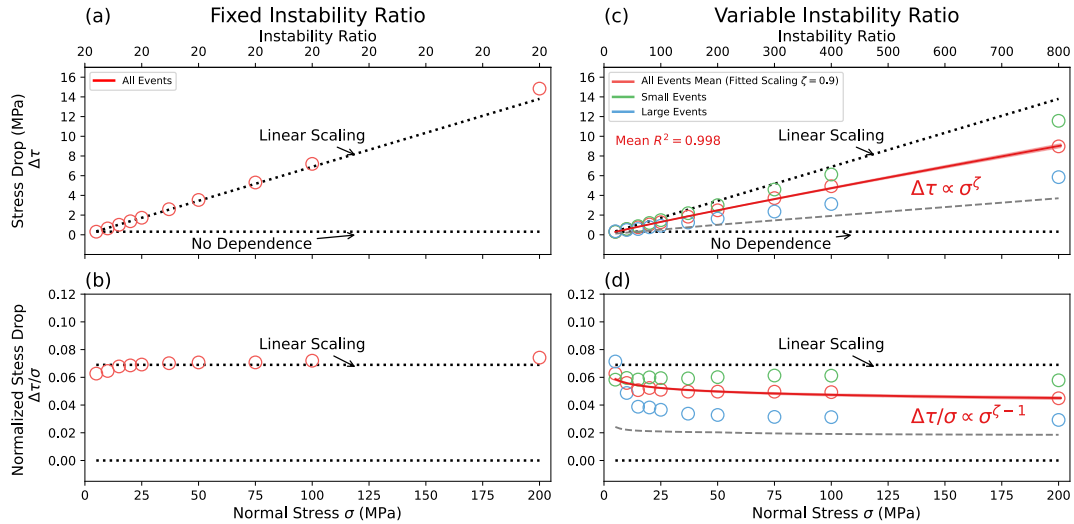

Figure 4. Average stress drop in fault models with increasing fault normal stress with (a) and (b) the same instability ratio R_I demonstrating linear scaling, and (c, d) where R_I increases with fault normal stress, resulting in sublinear power-law-like scaling for all events mean (red dots), small events mean (green dots), and large events mean (blue dots), defined by the rupture length smaller or larger than 10-times nucleation scale. The red line and shaded zone represent the 95% confidence interval from bootstrapping tests of fitting. The gray dashed lines in (c, d) depict an extrapolation of the power-law-like scaling with increasing normal stress for higher instability ratios using a smaller characteristic slip distance (Text S3 and Figure S6 in Supporting Information S1). The reference linear scaling is defined by Equation 2 using parameters in Table S1 of Supporting Information S1 and a dynamic slip rate of 10^{-3} m/s.

nucleation scale. For small events, a considerable portion of ruptured area has prestress levels closer to the quasi-static strength, which is more directly influenced by normal stress.

4. Discussion and Conclusions

We explored the relationship between average stress drop and fault normal stress in continuum fault models governed by standard rate-and-state friction. We found that models have a weaker dependence of stress drop on normal stress at large ratios of fault length to the nucleation scale (large R_I), which can be well-fit by a power-law with an exponent less than one. The power-law dependence that is weaker than the linearity predicted by the simple Coulomb friction model indicates the dependence is increasingly weaker at larger R_I. This result is more pronounced for large events with rupture length much larger than the nucleation scales. This arises in our models as earthquakes grow larger relative to their nucleation size and their averaged behavior is increasingly dominated by conditions for rupture propagation, which reflect more heterogeneous prestress conditions that are generally lower than the quasi-static fault strength.

We examined fault models with increasing normal stress in the parameter space of R_I up to ~800 as higher values of R_I are prohibitively computationally expensive. We found that average stress drop also decreases in models with higher instability ratios due to decreasing characteristic slip distance D_{RS}, for a fixed normal stress (Figure S6 in Supporting Information S1). The decrease in average stress drop with decreasing D_{RS} also exhibits a power-law-like scaling relation with an exponent around −0.1, consistent with the difference between linearity and the sublinear power-law scaling due to increasing normal stress. Should the scaling behavior in our models hold, our results predict that the dependence of average stress drop on normal stress asymptotically approaches zero for increasingly larger fault dimensions, and correspondingly large earthquakes, relative to their nucleation scale.

Natural faults commonly have a large range of earthquake sizes. Such faults are appropriately modeled by large instability ratios, which may partly explain the lack of an inferred depth dependence of earthquake stress drops. A fault with a characteristic dimension of tens of kilometers and a nucleation scale of 1 m, consistent with observations from meter-scale laboratory experiments (McLaskey, 2019) would correspond with R_I for natural faults around ~10^5. Extrapolating our results to higher instability ratios (R_I from 20,000 to 400,000) suggests that

natural fault conditions may fall in the even flatter portion of the power-law relation (gray lines in Figures 4c and 4d, Text S3 in Supporting Information S1).

Given observational limitations, stress drops for small earthquakes (e.g., $M < 1$–2) are challenging to reliably estimate (Allmann & Shearer, 2007). Observed scaling relations for earthquake stress drops may thus reflect events that are larger than the smallest events hosted by their corresponding faults. As such, seismological inferences may be more consistent with the even weaker scaling relation observed for our simulated ruptures that grow considerably larger than their nucleation scale (blue dots in Figure 4c, Figure S5 in Supporting Information S1), which could further contribute to the inferred depth-independence of stress drop.

Our models consider rupture sequences on a single planar fault segment where shear stress heterogeneity arises due to varying fault motion with spatially uniform properties. Models with depth-increasing normal stress and hence depth-increasing instability ratio suggest that the shear stress and seismicity distributions along faults may also be depth-dependent. This in turn could predict depth-dependent seismicity trends, including microseismicity and earthquake frequency-magnitude statistics (Figures 1f and 1g). However, additional forms of depth-dependent fault heterogeneity may influence fault behavior, including variable lithology (Ito & Kaneko, 2023; Skarbek et al., 2012), structural segmentation, and thermo-hydro-mechanical processes (Perry et al., 2020). Further work is warranted to examine our findings and the role of other forms of heterogeneity in 3D fully dynamic models.

Conflict of Interest

The authors declare no conflicts of interest relevant to this study.

Data Availability Statement

The simulated data and the code used in this study can be found at Yang et al. (2025).

Acknowledgments
The work of M.Y. & E.B. was supported by the U.S. Department of Energy, Office of Science, Office of Basic Energy Sciences, Heavy Element Chemistry program under Award Number DE-SC0023097. The work of V.L. was supported by NSF EAR- 2419373. We thank members of the UCSC Seismology Group for fruitful discussions. Figures are plotted using Matplotlib (Hunter, 2007).

References

Abercrombie, R. E. (2021). Resolution and uncertainties in estimates of earthquake stress drop and energy release. *Philosophical Transactions of the Royal Society A: Mathematical, Physical and Engineering Sciences*, *379*(2196), 20200131. https://doi.org/10.1098/rsta.2020.0131

Abercrombie, R. E., & Baltay, A. (2025). Magnitude, depth, and methodological variations of spectral stress drop within the SCEC/USGS community stress drop validation study using the 2019 ridgecrest earthquake sequence. *Bulletin of the Seismological Society of America*, *115*(6), 2741–2768. https://doi.org/10.1785/0120250056

Abercrombie, R. E., Baltay, A., Chu, S., Taira, T., Bindi, D., Boyd, O. S., et al. (2025). Overview of the SCEC/USGS community stress drop validation study using the 2019 ridgecrest earthquake sequence. *Bulletin of the Seismological Society of America*, *115*(3), 734–759. https://doi.org/10.1785/0120240158

Abercrombie, R. E., Trugman, D. T., Shearer, P. M., Chen, X., Zhang, J., Pennington, C. N., et al. (2021). Does earthquake stress drop increase with depth in the crust? *Journal of Geophysical Research: Solid Earth*, *126*(10), e2021JB022314. https://doi.org/10.1029/2021JB022314

Allmann, B. P., & Shearer, P. M. (2007). Spatial and temporal stress drop variations in small earthquakes near Parkfield, California. *Journal of Geophysical Research*, *112*(B4). https://doi.org/10.1029/2006JB004395

Allmann, B. P., & Shearer, P. M. (2009). Global variations of stress drop for moderate to large earthquakes. *Journal of Geophysical Research*, *114*(B1). https://doi.org/10.1029/2008JB005821

Barbot, S. (2019). Slow-slip, slow earthquakes, period-two cycles, full and partial ruptures, and deterministic chaos in a single asperity fault. *Tectonophysics*, *768*, 228171. https://doi.org/10.1016/j.tecto.2019.228171

Beeler, N., Kilgore, B., McGarr, A., Fletcher, J., Evans, J., & Baker, S. R. (2012). Observed source parameters for dynamic rupture with non-uniform initial stress and relatively high fracture energy. *Journal of Structural Geology*, *38*, 77–89. https://doi.org/10.1016/j.jsg.2011.11.013

Bilek, S. L., & Lay, T. (1999). Rigidity variations with depth along interplate megathrust faults in subduction zones. *Nature*, *400*(6743), 443–446. https://doi.org/10.1038/22739

Bindi, D., Spallarossa, D., Picozzi, M., Oth, A., Morasca, P., & Mayeda, K. (2023). The community stress-drop validation study—Part II: Uncertainties of the source parameters and stress drop analysis. *Seismological Research Letters*. https://doi.org/10.1785/0220230020

Brace, W. F., & Byerlee, J. D. (1966). Stick-slip as a mechanism for earthquakes. *Science*, *153*(3739), 990–992. https://doi.org/10.1126/science.153.3739.990

Brune, J. N. (1970). Tectonic stress and the spectra of seismic shear waves from earthquakes. *Journal of Geophysical Research (1896-1977)*, *75*(26), 4997–5009. https://doi.org/10.1029/JB075i026p04997

Cattania, C. (2019). Complex earthquake sequences on simple faults. *Geophysical Research Letters*, *46*(17–18), 10384–10393. https://doi.org/10.1029/2019GL083628

Dieterich, J. H. (1979). Modeling of rock friction: 1. Experimental results and constitutive equations. *Journal of Geophysical Research*, *84*(B5), 2161–2168. https://doi.org/10.1029/JB084iB05p02161

Huang, Y., Ellsworth, W. L., & Beroza, G. C. (2017). Stress drops of induced and tectonic earthquakes in the central United States are indistinguishable. *Science Advances*, *3*(8), e1700772. https://doi.org/10.1126/sciadv.1700772

Hunter, J. D. (2007). Matplotlib: A 2D graphics environment. *Computing in Science and Engineering*, *9*(3), 90–95. https://doi.org/10.1109/MCSE.2007.55

Ito, R., & Kaneko, Y. (2023). Physical mechanism for a temporal decrease of the gutenberg-richter *b* -value prior to a large earthquake. *Journal of Geophysical Research: Solid Earth*, *128*(12), e2023JB027413. https://doi.org/10.1029/2023JB027413

Kanamori, H., & Anderson, D. L. (1975). Theoretical basis of some empirical relations in seismology. *Bulletin of the Seismological Society of America*, *65*(5), 1073–1095. https://doi.org/10.1785/BSSA0650051073

Kaneko, Y., & Shearer, P. M. (2015). Variability of seismic source spectra, estimated stress drop, and radiated energy, derived from cohesive-zone models of symmetrical and asymmetrical circular and elliptical ruptures. *Journal of Geophysical Research: Solid Earth*, *120*(2), 1053–1079. https://doi.org/10.1002/2014JB011642

Lambert, V., & Lapusta, N. (2021). Resolving simulated sequences of earthquakes and fault interactions: Implications for physics-based seismic hazard assessment. *Journal of Geophysical Research: Solid Earth*, *126*(10), e2021JB022193. https://doi.org/10.1029/2021JB022193

Lambert, V., Lapusta, N., & Faulkner, D. (2021). Scale dependence of earthquake rupture prestress in models with enhanced weakening: Implications for event statistics and inferences of fault stress. *Journal of Geophysical Research: Solid Earth*, *126*(10), e2021JB021886. https://doi.org/10.1029/2021JB021886

Lambert, V., Lapusta, N., & Perry, S. (2021). Propagation of large earthquakes as self-healing pulses or mild cracks. *Nature*, *591*(7849), 252–258. https://doi.org/10.1038/s41586-021-03248-1

Lapusta, N., & Rice, J. R. (2003). Nucleation and early seismic propagation of small and large events in a crustal earthquake model. *Journal of Geophysical Research B*, *108*(B4), 2205. https://doi.org/10.1029/2001JB000793

Lapusta, N., Rice, J. R., Ben-Zion, Y., & Zheng, G. (2000). Elastodynamic analysis for slow tectonic loading with spontaneous rupture episodes on faults with rate- and state-dependent friction. *Journal of Geophysical Research*, *105*(B10), 23765–23789. https://doi.org/10.1029/2000JB900250

Lay, T., Kanamori, H., Ammon, C. J., Koper, K. D., Hutko, A. R., Ye, L., et al. (2012). Depth-varying rupture properties of subduction zone megathrust faults. *Journal of Geophysical Research*, *117*(B4). https://doi.org/10.1029/2011JB009133

Liu, Y., & Rice, J. R. (2005). Aseismic slip transients emerge spontaneously in three-dimensional rate and state modeling of subduction earthquake sequences. *Journal of Geophysical Research*, *110*(B8). https://doi.org/10.1029/2004JB003424

McLaskey, G. C. (2019). Earthquake initiation from laboratory observations and implications for foreshocks. *Journal of Geophysical Research: Solid Earth*, *124*(12), 12882–12904. https://doi.org/10.1029/2019JB018363

Noda, H., Dunham, E. M., & Rice, J. R. (2009). Earthquake ruptures with thermal weakening and the operation of major faults at low overall stress levels. *Journal of Geophysical Research*, *114*(B7). https://doi.org/10.1029/2008JB006143

Noda, H., Lapusta, N., & Kanamori, H. (2013). Comparison of average stress drop measures for ruptures with heterogeneous stress change and implications for earthquake physics. *Geophysical Journal International*, *193*(3), 1691–1712. https://doi.org/10.1093/gji/ggt074

Okubo, P. G., & Dieterich, J. H. (1984). Effects of physical fault properties on frictional instabilities produced on simulated faults. *Journal of Geophysical Research*, *89*(B7), 5817–5827. https://doi.org/10.1029/JB089iB07p05817

Oth, A., Miyake, H., & Bindi, D. (2017). On the relation of earthquake stress drop and ground motion variability. *Journal of Geophysical Research: Solid Earth*, *122*(7), 5474–5492. https://doi.org/10.1002/2017JB014026

Perry, S. M., Lambert, V., & Lapusta, N. (2020). Nearly magnitude-invariant stress drops in simulated crack-like earthquake sequences on rate-and-state faults with thermal pressurization of pore fluids. *Journal of Geophysical Research: Solid Earth*, *125*(3), e2019JB018597. https://doi.org/10.1029/2019JB018597

Rice, J. R. (1993). Spatio-temporal complexity of slip on a fault. *Journal of Geophysical Research*, *98*(B6), 9885–9907. https://doi.org/10.1029/93JB00191

Rice, J. R. (2006). Heating and weakening of faults during earthquake slip. *Journal of Geophysical Research*, *111*(B5). https://doi.org/10.1029/2005JB004006

Rubin, A. M., & Ampuero, J.-P. (2005). Earthquake nucleation on (aging) rate and state faults. *Journal of Geophysical Research*, *110*(B11). https://doi.org/10.1029/2005JB003686

Ruina, A. (1983). Slip instability and state variable friction laws. *Journal of Geophysical Research*, *88*(B12), 10359–10370. https://doi.org/10.1029/JB088iB12p10359

Scholz, C. H. (1998). Earthquakes and friction laws. *Nature*, *391*(6662), 37–42. https://doi.org/10.1038/34097

Shearer, P. M., Abercrombie, R. E., & Trugman, D. T. (2022). Improved stress Drop Estimates for M 1.5 to 4 earthquakes in Southern California from 1996 to 2019. *Journal of Geophysical Research: Solid Earth*, *127*(7), e2022JB024243. https://doi.org/10.1029/2022JB024243

Shearer, P. M., Prieto, G. A., & Hauksson, E. (2006). Comprehensive analysis of earthquake source spectra in southern California. *Journal of Geophysical Research*, *111*(B6). https://doi.org/10.1029/2005JB003979

Skarbek, R. M., Rempel, A. W., & Schmidt, D. A. (2012). Geologic heterogeneity can produce aseismic slip transients. *Geophysical Research Letters*, *39*(21), 2012GL053762. https://doi.org/10.1029/2012GL053762

Song, J. Y., & McLaskey, G. C. (2024). Laboratory earthquake ruptures contained by velocity strengthening fault patches. *Journal of Geophysical Research: Solid Earth*, *129*(4), e2023JB028509. https://doi.org/10.1029/2023JB028509

Steinhardt, W., & Brodsky, E. E. (2025). Precursory locking precedes slip events on laboratory fault. *Geophysical Research Letters*, *52*(4), e2024GL112882. https://doi.org/10.1029/2024GL112882

Steinhardt, W., Dillavou, S., Agajanian, M., Rubinstein, S. M., & Brodsky, E. E. (2023). Seismological stress drops for confined ruptures are invariant to normal stress. *Geophysical Research Letters*, *50*(9), e2022GL101366. https://doi.org/10.1029/2022GL101366

Trugman, D. T. (2020). Stress-drop and source scaling of the 2019 Ridgecrest, California, earthquake sequence. *Bulletin of the Seismological Society of America*, *110*(4), 1859–1871. https://doi.org/10.1785/0120200009

Trugman, D. T., & Shearer, P. M. (2017). Application of an improved spectral decomposition method to examine earthquake source scaling in Southern California. *Journal of Geophysical Research: Solid Earth*, *122*(4), 2890–2910. https://doi.org/10.1002/2017JB013971

Vallée, M. (2013). Source time function properties indicate a strain drop independent of earthquake depth and magnitude. *Nature Communications*, *4*, 2606. https://doi.org/10.1038/ncomms3606

Wu, Y., & Chen, X. (2014). The scale-dependent slip pattern for a uniform fault model obeying the rate- and state-dependent friction law. *Journal of Geophysical Research: Solid Earth*, *119*(6), 4890–4906. https://doi.org/10.1002/2013JB010779

Yang, M., Lambert, V., & Brodsky, E. E. (2025). The role of normal stress and shear stress heterogeneity in the inferred depth-independence of stress drop [Dataset]. *Zenodo*. https://doi.org/10.5281/zenodo.16050220

References From the Supporting Information

Day, S. M., Dalguer, L. A., Lapusta, N., & Liu, Y. (2005). Comparison of finite difference and boundary integral solutions to three-dimensional spontaneous rupture. *Journal of Geophysical Research*, *110*(B12). https://doi.org/10.1029/2005JB003813

Dieterich, J. H. (1992). Earthquake nucleation on faults with rate-and state-dependent strength. *Tectonophysics*, *211*(1), 115–134. https://doi.org/10.1016/0040-1951(92)90055-B

Dieterich, J. H., & Kilgore, B. D. (1994). Direct observation of frictional contacts: New insights for state-dependent properties. *Pure and Applied Geophysics PAGEOPH*, *143*(1–3), 283–302. https://doi.org/10.1007/BF00874332

Erickson, B. A., Jiang, J., Barall, M., Lapusta, N., Dunham, E. M., Harris, R., et al. (2020). The community code verification exercise for simulating sequences of earthquakes and aseismic slip (SEAS). *Seismological Research Letters*, *91*(2A), 874–890. https://doi.org/10.1785/0220190248

Jiang, J., Erickson, B. A., Lambert, V. R., Ampuero, J.-P., Ando, R., Barbot, S. D., et al. (2022). Community-driven code comparisons for three-dimensional dynamic modeling of sequences of earthquakes and aseismic slip. *Journal of Geophysical Research: Solid Earth*, *127*(3), e2021JB023519. https://doi.org/10.1029/2021JB023519

Marone, C. (1998). Laboratory-derived friction laws and their application to seismic faulting. *Annual Review of Earth and Planetary Sciences*, *26*(1), 643–696. https://doi.org/10.1146/annurev.earth.26.1.643

Noda, H. (2021). Dynamic earthquake sequence simulation with a SBIEM without periodic boundaries. *Earth Planets and Space*, *73*(1), 137. https://doi.org/10.1186/s40623-021-01465-6

Rice, J. R., & Ruina, A. L. (1983). Stability of steady frictional slipping. *Journal of Applied Mechanics*, *50*(2), 343–349. https://doi.org/10.1115/1.3167042